Hindawi
Advances in Meteorology
Volume 2019, Article ID 7698171, 16 pages
https://doi.org/10.1155/2019/7698171

Research Article

Performance of Three Reanalysis Precipitation Datasets over the Qinling-Daba Mountains, Eastern Fringe of Tibetan Plateau, China

Gefei Wang,[1,2] Xiaowen Zhang,[1,2] and Shiqiang Zhang[1,2]

[1]*Shaanxi Key Laboratory of Earth Surface System and Environmental Carrying Capacity, Northwest University, Xi'an, Shaanxi Province, China*
[2]*College of Urban and Environmental Science, Northwest University, Xi'an, Shaanxi Province, China*

Correspondence should be addressed to Shiqiang Zhang; zhangsq@lzb.ac.cn

Received 27 June 2018; Revised 11 November 2018; Accepted 12 December 2018; Published 23 January 2019

Academic Editor: Stefano Dietrich

Evaluation of different reanalysis precipitation datasets is of great importance to understanding the hydrological processes and water resource management practice in the Qinling-Daba Mountains (QDM), located at the eastern fringe of the Tibetan Plateau. Although the evaluation of satellite precipitation data in this region has been performed, another kind of popular precipitation product-reanalysis dataset has not been assessed in depth. Three popular reanalysis precipitation datasets, including ERA-Interim Reanalysis of European Centre for Medium Forecasts (ERA-Interim), Japanese 55-year Reanalysis (JRA-55), and National Centers for Environmental Prediction/National Center for Atmospheric Research Reanalysis-1 (NCEP/NCAR-1) were evaluated against rain gauge data over the Qinling-Daba Mountains from 2000 to 2014 on monthly, seasonal, and annual scales. Different statistical measures based on the Correlation Coefficient (CC), relative BIAS (BIAS), Root-Mean-Square Error (RMSE), and Mean Absolute Error (MAE) were adopted to determine the performance of the above reanalysis datasets. Results show that ERA-Interim and JRA-55 have good performance on a monthly scale and annual scale. However, the NCEP/NCAR-1 has the least BIAS with the observed precipitation in annual scale in QDM. All reanalysis datasets performed better in spring, summer, and autumn than in winter. The advantages of involving more precipitation observation stations was probably the main reason of the different performance of three precipitation reanalysis products, and the benefit of a four-dimensional variational analysis model over a three-dimensional variational analysis model may be another reason. The evaluation suggested that ERA-Interim is more suitable for study the precipitation and water cycles in the QDM.

1. Introduction

As a major component of the hydrological and energy cycle, the spatial and temporal patterns of precipitation greatly impact land surface hydrological fluxes and states [1–3]. Precipitation has a number of applications in various disciplines and studies, such as hydrology and water cycle processes, snowfall estimation, and climate research [4]; thus, its accuracy is pertinent. Traditionally, surface observations from rain gauges are regarded as one of the most accurate measurements for precipitation at a point scale. However, surface observation networks are sparse in many developing countries [5] due to the high cost of establishing and maintaining infrastructure [6]. Precise and continuous information on precipitation remains a challenging task, especially in remote mountainous areas.

Over the past several decades, tremendous efforts have been made to measure and monitor precipitation [7], which facilitate and promote the development of numerous global and quasiglobal precipitation products, including satellite-based datasets and reanalysis-based products using input sources, such as ground-based observations and satellite estimates. Advantages offered by satellites encourage the precipitation retrievals through visible spectrometry (VIS)/infrared (IR), passive microwave, active microwave, and multisensors methods, which are the foundation of satellite-

based precipitation estimates [4]. Conversely, various observational data and numerical weather prediction products are fused and integrated by data assimilation systems to produce the reanalysis datasets [8]. Satellite-based estimates and reanalysis datasets both need to be evaluated against in situ observations and calibrated before being implemented into various applications [9].

Therefore, various research studies have been conducted to explore the performance of the different datasets on regional [10–14] and global scales [15, 16]. Many studies have found that the datasets agree well on large scales but exhibit obvious and marked differences in various regions. For instance, Janowiak et al. [17] compared National Centers for Environmental Prediction (NCEP)-National Center for Atmospheric Research (NCAR) reanalysis data and Global Precipitation Climatology Project (GPCP) rain gauge-satellite combined dataset globally over the period 1988–1995 and found good agreement between large-scale patterns but poor performance in some regional characteristics, such as oceans and equatorial land regions. Huffman et al. [18] and Kummerow et al. [19] explained the necessities for adequate validations on regional scales instead of using global approaches. Taking into account the above reasons, although Zhao and Fu [20], Ma et al. [21], and other researchers [22–24] have performed relevant studies in China, conclusions are still unclear on a regional scale. Therefore, it is necessary to validate and evaluate the performance of various precipitation datasets in certain areas, especially in mountainous areas.

The Qinling-Daba Mountains (QDM), which geographically and climatologically divide northern and southern China with the Huaihe River, serve as an important water source for the middle route of South-to-North Water Diversion Project in China. Meanwhile, the QDMs are located at the eastern fringe of the mountain region of the Qinghai Tibetan Plateau, which is the source of many large rivers and called "Asia Water Tower." Knowledge of precipitation in the QDM is of great significance to water resources management, hydrological modeling, and climate research in the immediate and surrounding regions. Given the large variations in the terrain, mountain systems develop considerably complex local and regional climate systems [25], which increase the difficulties in obtaining accurate precipitation information.

The development of precipitation datasets provides beneficial conditions to measure precipitation in the QDM. Ren et al. [26] evaluated the precipitation from the Tropical Rainfall Measuring Mission (TRMM 3B42) in the surrounding area. Wang et al. [27] assessed the performance of the Climate Prediction Center morphing technique (CMORPH), Global Precipitation Climatology Project (GPCP-2), TRMM 3B43, Global Precipitation Climatology Center (GPCC), and China Meteorological Forcing Data developed by the Institute of Tibetan Plateau Research, Chinese Academy of Sciences (ITPCAS) over the QDM and reclaimed that ITPCAS and TRMM 3B43 performed better overall. These results concentrated on satellite-based precipitation datasets. Another kind of precipitation product, reanalysis-based datasets, which integrate ground observation data and atmospheric models, provide an alternative perspective for understanding the spatial distribution of precipitation in mountainous areas where satellite data are difficult to cove or large errors exist. The reanalysis precipitation products have been commonly used in climatology and basin hydrometeorology [28–31], but have not been fully evaluated in the QDM.

The main objective of this work is to evaluate three reanalysis-based datasets on monthly, seasonal, and annual scales through observations in the QDM during 2000–2014. This paper is organized as follows: Section 2 describes the basic information of the study area; Section 3 introduces the relevant datasets and evaluation methods; Section 4 presents the evaluation results; Section 5 discusses the probable reason behind the different performances of the reanalysis datasets; and Section 6 summarizes the conclusions.

2. Study Area

The QDM, referring to both Qinling Mountain and Daba Mountain, are located in central China with an area of about 222,300 km^2, from 30°50′ N to 34°59′ N latitude and from 102°54′ E to 112°40′ E longitude (Figure 1) [32, 33]. This area is roughly consistent with 0°C isothermal contours in January, 800 mm isohyet curves, and annual 2000 h sunshine hour contour lines in China [34, 35]. The elevation in the QDM varies greatly, where the difference between the maximum and minimum elevation is almost 4000 m (Figure 1), and precipitation distributed with significant spatial and temporal heterogeneity. The main land cover of QDM is forest and shrub, where forest is mainly distributed in west of QDM and shrub mainly distributed in east of QDM. The soil texture has vertical zonal distribution from yellow clunamon soil at the foot of the mountains to mountain dark brown soil at the peak of the mountains. The spatial distribution of average of annual precipitation during 1958 to 2014 shows that the annual precipitation in the northwestern region is about 500 mm, which is far less than that in the southwestern areas (about 1300 mm) (Figure 2(a)). Meanwhile, the main seasonal pattern of rainfall suggests that the QDM have four distinct seasons, and precipitation mainly occurs during warmer months from May to September (Figure 2(b)).

3. Data and Methodology

3.1. Reanalysis Precipitation Datasets. ERA-Interim, JRA-55, and NCEP/NCAR-1, which are popular used in many studies [17, 21, 28–31] and are available to public, were chosen as the reanalysis dataset to be evaluated in this study.

ERA-Interim is a global reanalysis product created by European Center for Medium-Range Weather Forecasts (ECMWF) [36], which was initiated in 1979. This reanalysis dataset is carried out with a 4-Dimensional VARiational analysis (4D-VAR) data assimilation scheme, a better formulation of background error constraint, a new humidity analysis, and many other improvements, to address several difficult data assimilation problems encountered during the production of ERA-40 and achieve great progresses

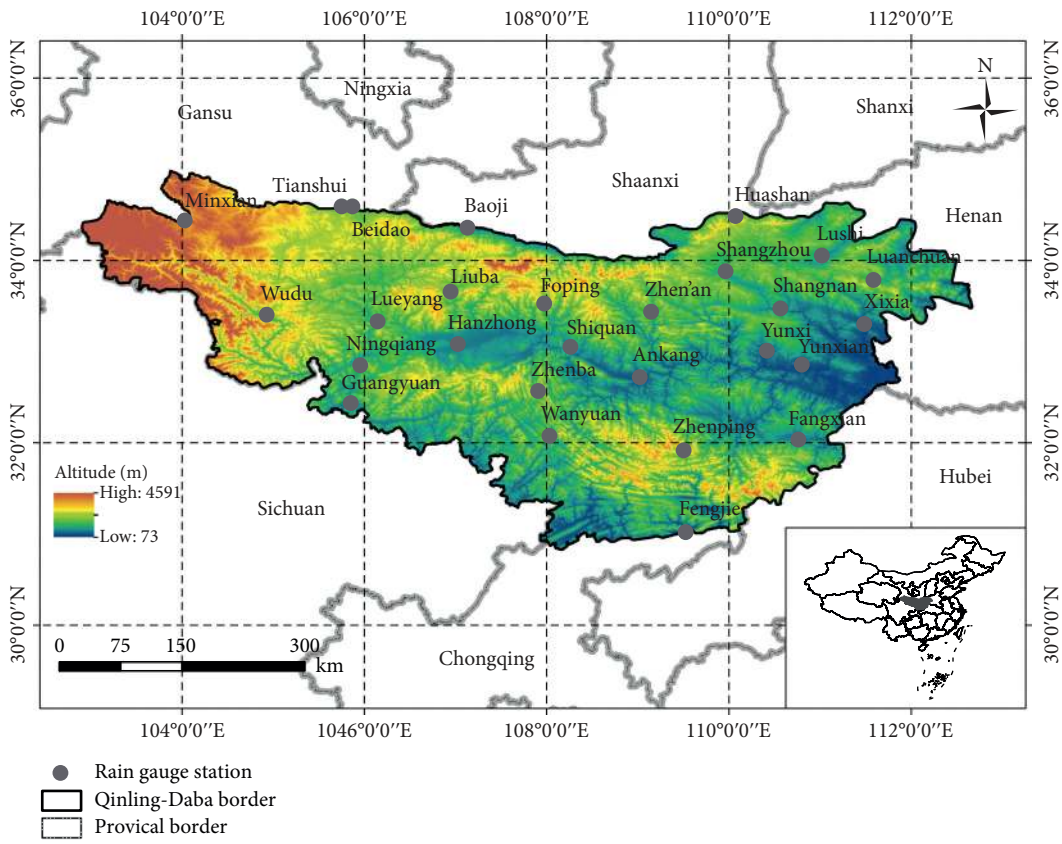

Figure 1: The location and the spatial distribution of the rain gauge stations over the Qinling-Daba Mountains in China (Figure 1 is reproduced from Wang et al. [27] under the Creative Commons Attribution License/public domain).

compared to ERA-40 [37]. The overwhelming majority of observation data, and most of the increase over time, originate from satellites. Such data include clear-sky radiance measurements from polar-orbiting and geostationary sounders and imagers, atmospheric motion vectors derived from geostationary satellites, scatterometer wind data, and ozone retrievals from various satellite-borne sensors. The total precipitable vapor estimates are also derived from satellite observations. Although manual and automatic ground observations of precipitation were also considered, the number of stations in the QDM involved in data assimilation is unclear. In this study, monthly ERA-Interim was obtained from ECMWF on a fixed grid of $0.75^\circ \times 0.75^\circ$ (http://apps.ecmwf.int/).

JRA-55 is a global reanalysis dataset constructed by the Japan Meteorological Agency (JMA) [38]. JRA-55 employs a 4D-VAR with variational bias correction for satellite radiances. It aims at providing a comprehensive atmospheric dataset that is suitable for studies on climate change and related issues [39]. The observation data primarily included conventional data (such as tropical cyclone wind retrievals, pilot balloons, wind profilers, etc.), wind data retrieved from geostationary TOVS (TIROS Operational Vertical Sounder), ATOVS (advanced TOVS), AMV (Atmospheric Motion Vector), CSR (Clear-Sky Radiance) data, and other remote sensing data [40]. Moreover, newly available observational datasets were collected and used whenever possible [41]. In this study, monthly data from JRA-55 were adopted, which are accessed for free online (http://jra.kishou.go.jp/).

NCEP/NCAR-1 is a global reanalysis dataset of atmosphere fields produced by the National Centers for Environmental Prediction and National Center for Atmospheric Research to meet the needs of research and climate monitoring communities [42]. A 3D-VAR (three-dimensional variational analysis) is used in the assimilation system of NCEP/NCAR-1. The horizontal resolution is T62 Gaussian grid with 192×94 grids of the overall dataset [8]. This model includes parametrizations of all major physical processes, such as convection, clouds, and an interactive surface hydrological model on a global scale. The NCEP/NCAR-1 precipitation field from short-range model forecast accumulations, but observed precipitation is not used in the assimilation phase of the model [43]. Monthly data from NCEP/NCAR-1 were used in this work, which can be downloaded online (https://www.esrl.noaa.gov/).

3.2. Gauged Precipitation Data. The China Meteorological Administration (CMA) provided daily in situ observational precipitation data over the QDM during 2000–2014. The precipitation is manually observed at 8 : 00 and 20 : 00 per day by a rain gauges without windproof fences, the area of the collector orifice is 200 cm^2, ground stations using the same criteria of CMA in the observation field with

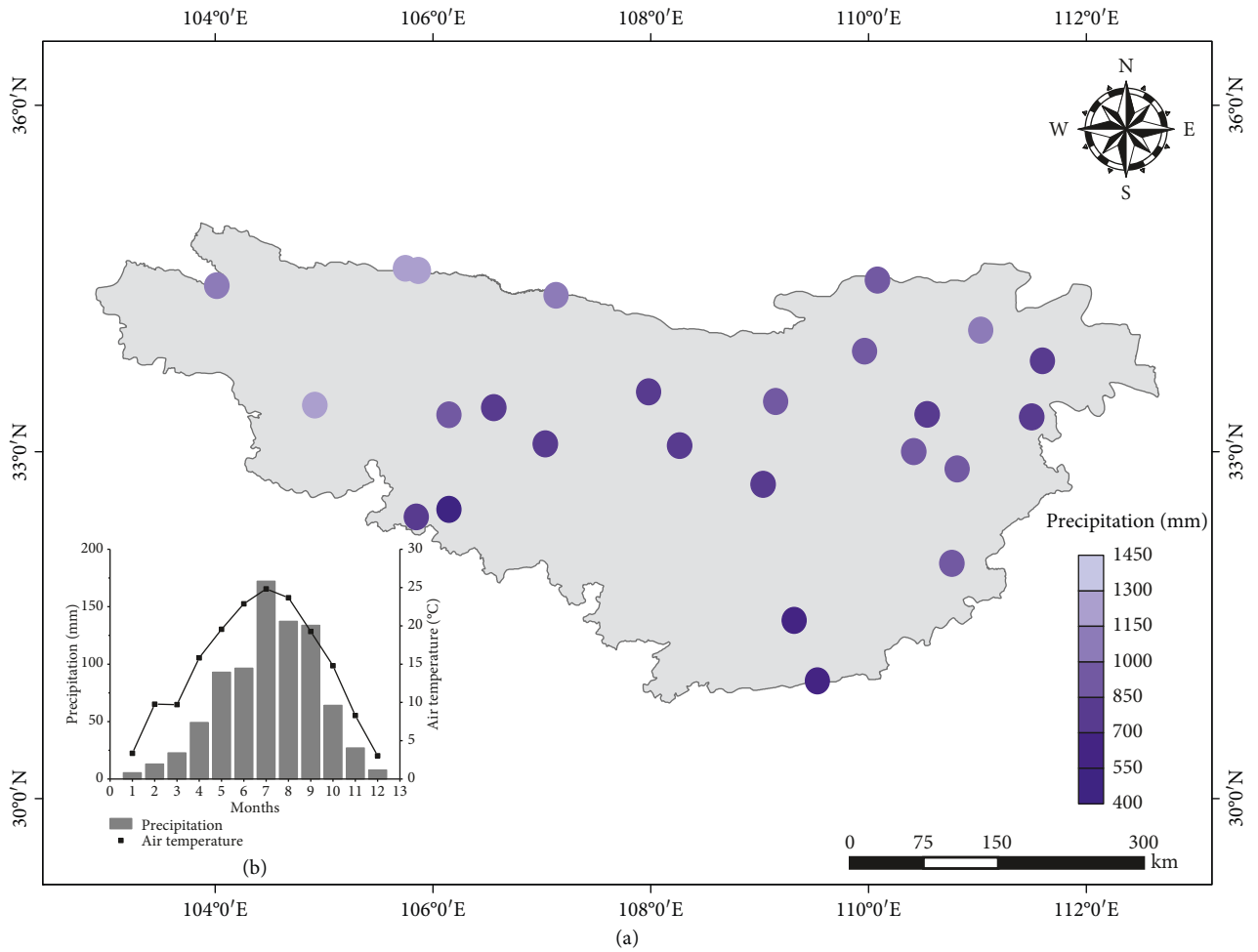

Figure 2: (a) The spatial distribution of annual rainfall; (b) the time distribution of monthly rainfall and air temperature throughout the year over the Qinling-Daba Mountains, China (Figure 2 is reproduced from Wang et al. [27], under the Creative Commons Attribution License/public domain).

25 m × 25 m with short grass cover, the gauge orifice is 0.7 m above surface. Snow collected in precipitation gauges was melted after each observation and then measured using a standard glass graduated measuring cylinder. Routine maintenance includes the gauge and the field [44].

A 0.1° buffer both in latitude and longitude direction of the study area boundary was utilized to ensure that the 27 chosen rain gauge stations were able to delineate relatively accurate spatial distribution of precipitation as much as possible [27]; 18 stations have continuous precipitation data from 2000–2014, while the remaining 9 stations do not. Therefore, 27 meteorological stations were used in the overall evaluation of monthly and annual precipitation, and 18 stations were used for circumstances requiring continuous time series. Manual quality control was carried out, and the gauged precipitation data were used as the reference data to evaluate the performance of reanalysis precipitation datasets in the study. Information and record periods of each gauge station are listed in Table 1.

3.3. Evaluation Method. In terms of temporal resolution, daily gauged precipitation data were accumulated to monthly and annual data. Meanwhile, the precipitation rate data from JRA-55 and NCEP/NCAR-1 were multiplied by corresponding times to obtain rainfall amount which is on the same time scale as gauged rainfall. The monthly total precipitation data of ERA-Interim were obtained by accumulating the daily precipitation. The seasonal total precipitation were summed from monthly precipitation, including winter precipitation (December, January, and February), spring precipitation (March, April, and May), summer precipitation (June, July, and August), and autumn precipitation (September, October, and November).

It is common practice in evaluation studies to compare the point-based rain gauge data against the grid-based precipitation datasets. Given the 18 stations with continuous time series over the QDM, a point-pixel comparison was performed in this study to avoid errors by gridding the rain gauge data [11, 45]. The rainfall values from each rain gauge and the grid where the same gauge is located were extracted in pairs for evaluation. Before that, ERA-Interim and JRA-55 were resampled to horizontal 0.5° × 0.5° grid scales to acquire a uniform spatial resolution by bilinear interpolation, which

Table 1: The basic information of gauge station over the Qinling-Daba Mountains, China.

Station name	Latitude (°)	Longitude (°)	Elevation (m a.s.l.)	Observation years
Minxian	34.43	104.02	2315	2000–2014
Wudu	33.4	104.92	1079	2000–2014
Tianshui	34.58	105.75	1142	2000–2003, 2007–2008
Beidao	34.57	105.87	1085	2004–2014
Baoji	34.35	107.13	612	2000–2004, 2007–2008
Huashan	34.48	110.08	2065	2000–2014
Lushi	34.05	111.03	569	2000–2014
Luanchuan	33.78	111.6	750	2000–2014
Lueyang	33.32	106.15	794	2000–2014
Liuba	33.65	106.95	1547	2009–2014
Hanzhong	33.07	107.03	510	2000–2014
Foping	33.52	107.98	827	2000–2014
Shangzhou	33.87	109.97	742	2000–2014
Zhen'an	33.43	109.15	694	2000–2014
Shangnan	33.46	110.58	1137	2009–2014
Xixia	33.3	111.5	250	2000–2014
Guangyuan	32.43	105.85	514	2000–2014
Ningqiang	32.84	105.95	1400	2009–2014
Shiquan	33.05	108.27	485	2000–2014
Wanyuan	32.07	108.03	674	2000–2014
Zhenba	32.56	107.91	1231	2009–2014
Ankang	32.72	109.03	291	2000–2014
Yunxi	33	110.42	249	2000–2014
Yunxian	32.85	110.82	202	2007–2008
Fangxian	32.03	110.77	427	2000–2014
Zhenping	31.91	109.51	1615	2009–2014
Fengjie	31.02	109.53	300	2000–2014

is a popular method in meteorology and climate studies [46, 47]. However, considering the unequal spacing between x and y coordinates between the grid points of NCEP/NCAR-1, resampling will introduce errors. Therefore, rain gauge data were directly compared against the nearest grid points of NCEP/NCAR-1 in the original resolution without resampling.

To quantitatively assess the performance of ERA-Interim, JRA-55, and NCEP/NCAR-1 in the QDM, the following several statistical indices were obtained and compared:

$$\begin{aligned}
\mathrm{CC} &= \frac{\sum_{i=1}^{n}\left(G_i-\overline{\overline{G}}\right)\left(P_i-\overline{\overline{P}}\right)}{\sqrt{\sum_{i=1}^{n}\left(G_i-\overline{\overline{G}}\right)^2\left(P_i-\overline{\overline{P}}\right)^2}},\\
\mathrm{BIAS} &= \frac{\sum_{i=1}^{n}\left(G_i-P_i\right)}{\sum_{i=1}^{n}G_i}\times 100\%,\\
\mathrm{RMSE} &= \sqrt{\frac{1}{n}\sum_{i=1}^{n}\left(G_i-P_i\right)^2},\\
\mathrm{MAE} &= \frac{1}{n}\sum_{i=1}^{n}\left|G_i-P_i\right|,
\end{aligned} \tag{1}$$

where n is the total number of samples; G_i represents the gauged precipitation at ith month; P_i is the precipitation at ith month from reanalysis precipitation datasets; and $\overline{\overline{G}}$ and $\overline{\overline{P}}$ are the average values over n months of G_i and P_i, respectively. The Pearson correlation coefficient (CC) has no units and is used to assess the degree of agreement that reflects the level of linear correlation, which varies from −1 to 1, where positive and negative values indicate positive and negative correlation, respectively. The relative bias (BIAS) provides information on the magnitude of underestimation or overestimation between two datasets, in which the closer to 0 the BIAS is, the better performance the precipitation dataset has. The root-mean-square error (RMSE) is sensitive to the maximum and minimum values, and the mean absolute error (MAE) demonstrates the magnitude of mean error. The different indices all used in conjunction to determine the performance of the reanalysis precipitation datasets.

Given the emphasis in multiple related studies on assessment of precipitation products [9, 48], CC is regarded as the primary and principle indicator to evaluate the accuracy of precipitation products at various circumstances. The T-test is also performed to verify the statistical significance of CC in advance [49, 50] after checking if the data are normally distributed. BIAS is used to determine the scale of underestimation or overestimation for true precipitation, while RMSE and MAE are utilized to measure the specific errors of the precipitation products.

The absolute precipitation differences (PD) and percentage of PD (PPD) were adopted as two different methods to quantitatively determine the agreement between precipitation datasets and gauge data during the dry and wet years:

$$\begin{aligned} \mathrm{PD} &= \text{estimated} - \text{observed}, \\ \mathrm{PPD} &= \frac{\text{estimated} - \text{observed}}{\text{observed}} \times 100\%. \end{aligned} \tag{2}$$

3.4. Precipitation Centroid. The spatial pattern of the precipitation and its temporal change is one of the characteristics of regional precipitation and hydrological process. Traditional spatial evaluation of precipitation products directly compares the spatial distribution of rainfall, which lack quantitative descriptions. Therefore, this study implemented precipitation centroid movement over a 15-year period from 2000 to 2014 to further explore the effectiveness of ERA-Interim, JRA-55, and NCEP/NCAR-1.

A centroid, which stems from the concept of center of mass (or gravity) in physics, was first introduced in humanities and social fields, such as population, economy, and tourism [51–54] and has recently been applied to measure precipitation spatial heterogeneity [55, 56]. The precipitation centroid is defined as the point where the moment of precipitation reaches balance in the space plane of the study area that reflects the spatial distribution of precipitation [48], which is introduced to further determine the difference between gauge observation and ERA-Interim, JRA-55, and NCEP/NCAR-1. The moving trajectory of the precipitation centroid displays the change in the spatial distribution of precipitation, which means the similarity between precipitation from products and gauges can be used to verify their spatial heterogeneity agreement [55, 56]. Furthermore, the distance between precipitation centroids of two adjacent years is regarded as the migration distance, and the total migration distances are compared to quantitatively measure the precision of precipitation datasets. We use the migration distance between adjacent years to quantitatively determine the performance of the three reanalysis precipitation datasets.

Coordinates of the precipitation centroid were calculated using the following formulas:

$$\begin{aligned} X &= \frac{\sum_{i=1}^{n} P_i x_i}{\sum_{i=1}^{n} P_i}, \\ Y &= \frac{\sum_{i=1}^{n} P_i y_i}{\sum_{i=1}^{n} P_i}, \end{aligned} \tag{3}$$

where n is the number of the rain gauge stations; the location of a rain gauge is (x_i, y_i); and P represents the amount of precipitation from observation and precipitation products.

4. Evaluation Results

The performance of ERA-Interim, JRA-55, and NCEP/NCAR-1 on monthly, seasonal, and annual scales is presented in this section. In this study, the monthly scale was used as the base time scale, and movement of the precipitation centroid was analyzed to further explore the performance of the three datasets over the QDM, China.

4.1. Performance on Monthly Scale. Three reanalysis precipitation datasets were first validated on a monthly scale. To eliminate the influence of the seasonal cycle on CC, the CC of each precipitation dataset was calculated per month (Figure 3). All datasets passed the significance test at the 99% confidence level except NCEP/NCAR-1 in certain months. It is clear that ERA-Interim outperformed the other reanalysis precipitation products in most months and had an average CC of 0.64. JRA-55 performed second-best with a mean CC of 0.58. Meanwhile, JRA-55 was better than ERA-Interim in June, July, August, and September, and ERA-Interim had higher agreement with observed precipitation than JRA-55 in the remaining eight months. In addition, JRA-55 simulated precipitation better in months with abundant rainfall. NCEP/NCAR-1 performed worst with the lowest CC (about 0.22) among the evaluated precipitation datasets.

Therefore, the average CCs of the twelve months of a specific year were treated as the overall performance of every single precipitation product on a monthly scale, which are shown in Table 2 with the other evaluation indices.

Overall, ERA-Interim and JRA-55 revealed a similar ability to simulate rainfall for evaluation indices. ERA-Interim had better CC and MAE, and JRA-55 had a better BIAS and RMSE. NCEP/NCAR-1 had the lowest CC and largest RMSE and MAE, suggesting that NCEP/NCAR-1 is the poor performing dataset, even though it had a low BIAS.

The spatial distribution of evaluation indices at individual gauges was obtained to investigate the performance of the three precipitation products, as illustrated in Figures 4 and 5.

The spatial distribution of correlation coefficients suggests that CCs at most sites were greater than 0.5 for ERA-Interim and JRA-55 (Figure 4). ERA-Interim and JRA-55 have the same number of stations with CC values higher than 0.7. NCEP/NCAR-1 (Figure 4(c)) showed the worst performance with lower CCs at most stations, where five stations even had CC values lower than 0.5.

Furthermore, stations with relatively high CCs were concentrated in the northeastern region of the QDM, which due to the relatively low altitude in the eastern region. The influence of terrain in the eastern region is less than the western and northwestern part of QDM. It is well established that the topographic and orographic influences on precipitation formation and propagation. It is expected that there is less precipitation on the leeward side of the mountain on the western side of the QDM because of the dry-adiabatic decent of air, which leads to lower CCs. It is worth noting that ERA-Interim and JRA-55 had the lowest CC at Wudu station at the same time.

ERA-Interim and JRA-55 had similar distributions of BIAS, which are both overestimated the precipitation at the most stations. Comparatively, NCEP/NCAR-1 underestimated rainfall. ERA-Interim, JRA-55, and NCEP/NCAR-1 all had the largest errors at Wudu station with positive BIAS values of 130.4%, 123.3%, and 223.4%, respectively, which may be attributed to the complex terrain in Bailongjiang Valley. Another interesting phenomenon was the underestimation of precipitation at Huashan station for ERA-Interim, JRA-55, and NCEP/NCAR-1. Considering

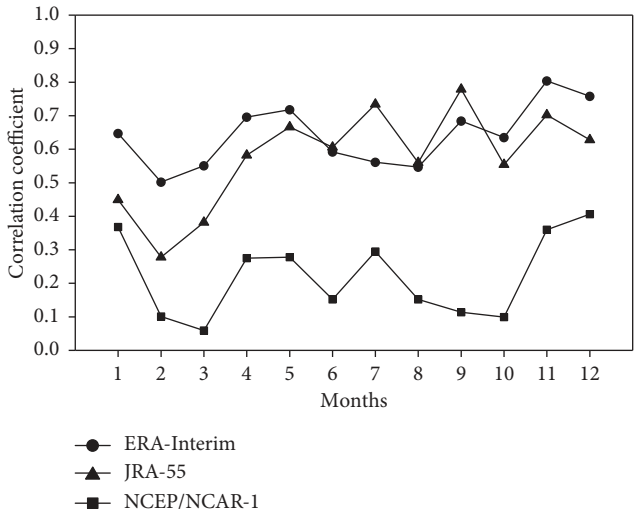

Figure 3: The line chart of correlation coefficient (CC) between monthly observed precipitation and ERA-Interim, JRA-55, and NCEP/NCAR-1 precipitation during 2000 to 2014 over the Qinling-Daba Mountains, China.

Table 2: The average of CC, BIAS, RMSE, and MAE between three reanalysis precipitation datasets and gauged precipitation data on a monthly scale during 2000 to 2014 over the Qinling-Daba Mountains, China.

Index	ERA-Interim	JRA-55	NCEP/NCAR-1
CC	0.64	0.58	0.22
BIAS (%)	21.78	16.57	−6.31
RMSE (mm)	48.56	43.05	64.93
MAE (mm)	30.42	30.81	39.18

that the elevation of Huashan station is 2054 m a.s.l., the large wind at such a high elevation leads to lower precipitation gauge capture rate [57], and precipitation of reanalysis products is expected to be overestimated. However, it is difficult to determine the contribution of the underestimation of observed precipitation and the overestimation of the reanalysis products, respectively.

4.2. Performance on Seasonal Scale. In this study, precipitation was greater during summer (June–August) and autumn (September–November) than in spring (March–May) and winter (December–next February) (Figure 2(b)). To understand the seasonal pattern of errors for reanalysis precipitation datasets comprehensively, the overall performance of ERA-Interim, JRA-55, and NCEP/NCAR-1 were evaluated and are shown in Table 3.

All reanalysis datasets displayed higher CC values in spring, summer, and autumn than winter and had lower BIAS values in summer and autumn than spring and winter. Thus, precipitation datasets performed better in warmer and wetter seasons (summer and autumn), which may be conducive to monitoring and predicting geologic hazards caused by heavy rain in a short time period in the QDM. The larger errors in RMSE and MAE in summer and autumn may be due to the fact that rainfall concentrated during those seasons over the QDM (Figure 2).

It is worth mentioning that JRA-55 coincided worse performing with observed rainfall in spring and winter but performed better in summer and autumn than ERA-Interim, which indicates that it may be better to use JRA-55 for simulating abundant precipitation than ERA-Interim over the QDM. The CCs of NCEP/NCAR-1 were too low to simulate true rainfall, making NCEP/NCAR-1 the worst performance dataset of the three.

In summary, all evaluated datasets displayed higher accuracy in summer and autumn than spring and, especially winter, when the performance of the datasets was much worse than the other seasons. ERA-Interim and JRA-55 had similar performance and good agreement with observed precipitation, while NCEP/NCAR-1 showing the poorest performance.

4.3. Performance on Annual Scale. The average annual precipitation of each dataset was calculated and compared with the in situ observed precipitation on an annual scale (Figure 6).

The annual precipitation was in continuous fluctuation from 2000 to 2014, and the overall trend of reanalysis datasets was consistent with the precipitation from rain gauges. However, some deviations were found for certain years: the observed rainfall reached a maximum and minimum value in 2011 and 2001, respectively, while ERA-Interim, JRA-55, and NCEP/NCAR-1 were not in agreement: ERA-Interim and JRA-55 peaked in 2003, which meant the rainfall simulation ability should be further enhanced. Meanwhile, changes in the performance of the reanalysis datasets may be related to improvements in algorithms and additional data in recent years.

A quantitative evaluation on an annual scale in the QDM is based on the overall performance of the three reanalysis precipitation datasets in Table 4.

From the evaluation indices, JRA-55 had higher accuracy than ERA-Interim at annual scale with slight advantages. NCEP/NCAR-1 had best BIAS value and worst CC, RMSE, and MAE. Considering the possible mutual cancellation in BIAS, NCEP/NCAR-1 was also regard as the worst product all in all.

The spatial distribution of CC for annual precipitation at each gauge over the QDM (Figure 7) suggests that ERA-Interim and JRA-55 had CCs beyond 0.5 as a whole, while NCEP/NCAR-1 showed the poorest CCs. Only three stations had CCs for NCEP/NCAR-1 bigger than 0.5, indicating that precipitation in this region cannot be represented on an annual scale. In addition, no obvious pattern was observed for correlation coefficients in the spatial distribution of NCEP/NCAR-1 (Figure 7(c)).

Comprehensively, the values of RMSE and MAE varied with the precipitation accumulation on monthly, seasonal, and annual scales. ERA-Interim and JRA-55 performed better on a monthly scale than an annual scale. On a monthly scale, ERA-Interim had a higher CC and lower MAE values than JRA-55, while JRA-55 had a lower BIAS and RMSE than ERA-

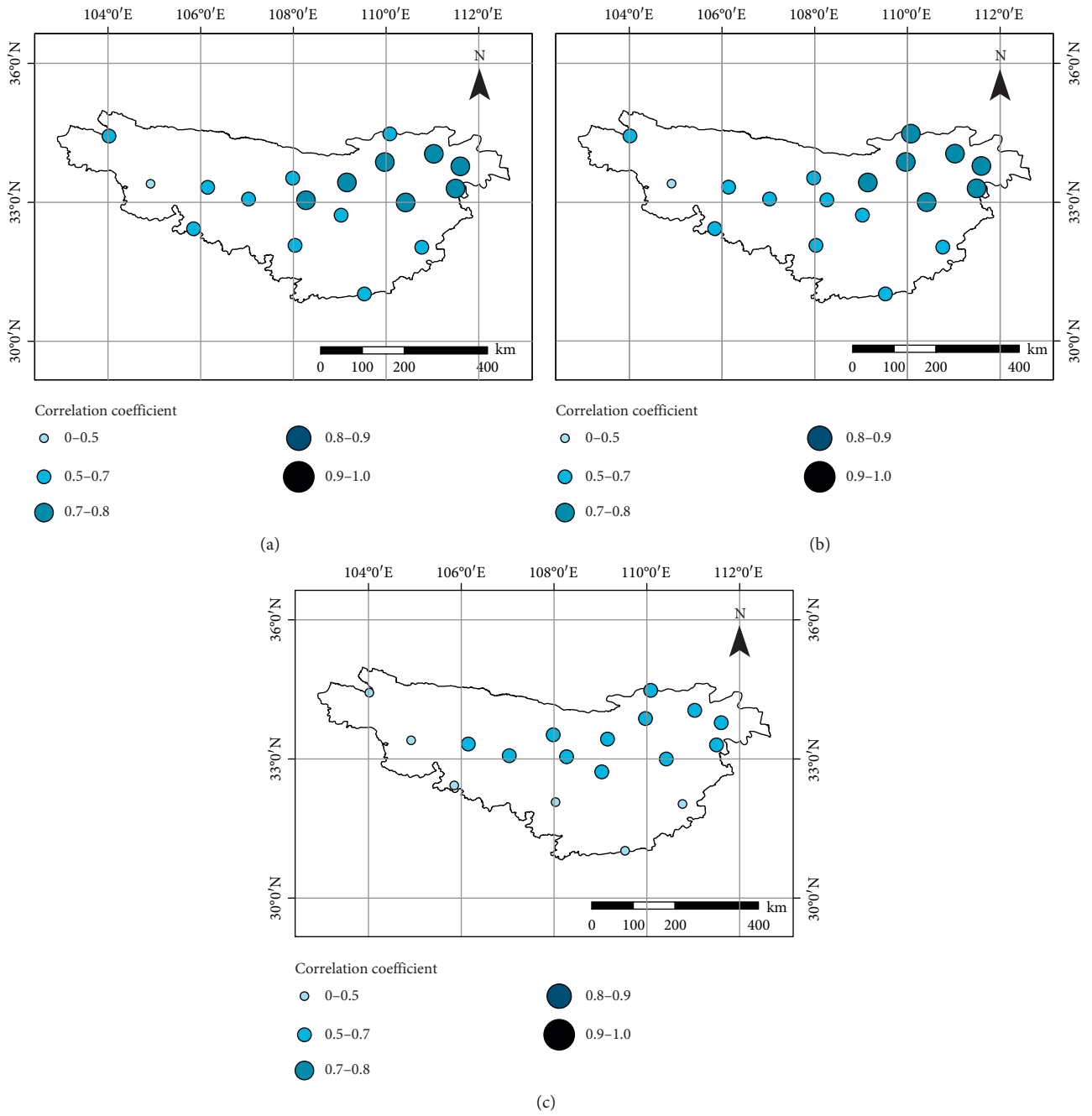

Figure 4: Correlation coefficient at each precipitation gauge stations over the Qinling-Daba Mountains for monthly precipitation between (a) ERA-Interim and gauges, (b) JRA-55 and gauges, and (c) NCEP/NCAR-1 and gauges.

Interim. The performance of ERA-Interim and JRA-55 is equally matched. However, JRA-55 was better than ERA-Interim for all indices on an annual scale. Further, ERA-Interim and JRA-55 exhibit a better ability to simulate precipitation in the spring, summer, and autumn than in winter.

4.4. Performance in the Wet and Dry Years. To further explore the performance of reanalysis precipitation datasets, based on whether the gauges average annual precipitation in the year is greater or less than the average during 2000 to 2014, the 15-year period was further divided into two groups: wet years and dry years. The wet years include 2000, 2003, 2005, 2009, 2010, 2011, and 2014; the other years between 2001 and 2014 belong to the dry years over the QDM. The PDs and PPDs during the wet and dry years are shown in Tables 5 and 6, respectively.

The PDs and PPDs for reanalysis precipitation datasets varied in the wet (Table 5) and dry years (Table 6). Overestimation was common during the wet and dry years for ERA-Interim and JRA-55. However, NCEP/NCAR-1 has smaller PDs and PDDs both in wet and dry years, especially

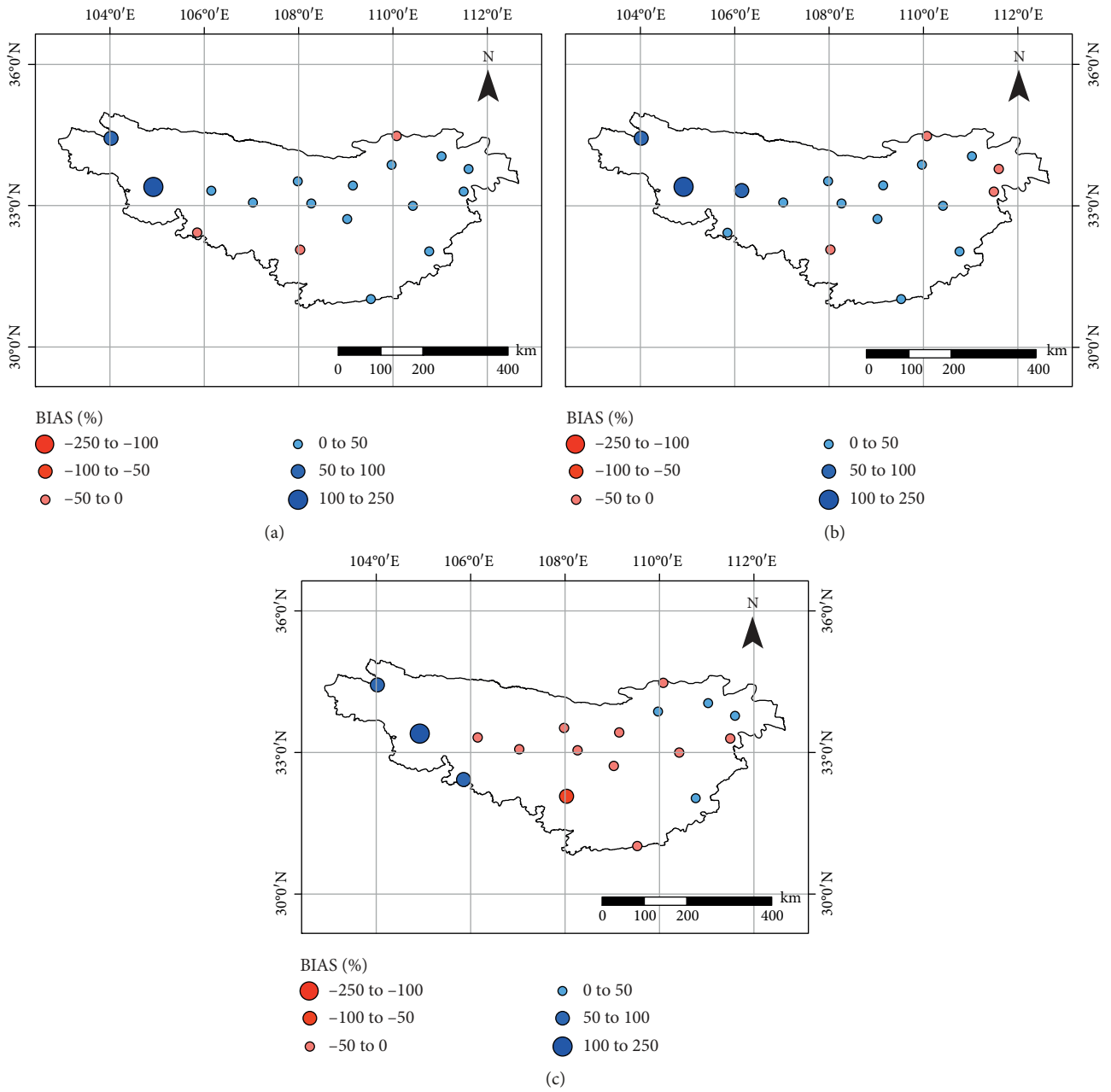

Figure 5: BIAS (%) at each gauge over the Qinling-Daba Mountains for monthly precipitation between (a) ERA-Interim and gauges, (b) JRA-55 and gauges, and (c) NCEP/NCAR-1 and gauges.

in wet years, indicating that it has more underestimated years during dry years than wet years.

4.5. Precipitation Centroid. The precipitation centroids of rain gauges and ERA-Interim, JRA-55, and NCEP/NCAR-1 reanalysis products were all located in the central region of the QDM and presented an east-west spatial distribution pattern (Figure 8). Visually, ERA-Interim (Figure 8(b)) displayed the best agreement with rain gauges due to a close spatial distribution pattern of centroid movement. Moreover, most precipitation centroids of JRA-55 (Figure 8(c)) and NCEP/NCAR-1 (Figure 8(d)) were generally located in the western parts compared with those of rain gauges, which indicated the largest discrepancy among them. According to the definition of precipitation centroid, the centroid will be closer to places with more abundant precipitation, which indicates that JRA-55 and NCEP/NCAR-1 may overestimate precipitation in western parts of QDM. It also can be found from the spatial distribution of BIAS on a monthly scale (Figure 5). The number of stations for large overestimations by JRA-55 and NCEP/NCAR-1 is more than those of ERA-Interim in the western parts of QDM.

The centroid movement distance is accumulated to estimate the magnitude of correspondence between reanalyzed and gauged data as an evaluation indicator (Table 7). The

Table 3: CC, BIAS, RMSE, and MAE between three reanalysis precipitation datasets and gauged precipitation data at the seasonal scale over the Qinling-Daba Mountains, China (all products passed the significance test at the 99% confidence level).

Season	Dataset	CC	BIAS (%)	RMSE (mm)	MAE (mm)
Spring	ERA-Interim	0.67	23.61	69.45	55.79
	JRA-55	0.51	35.61	89.65	71.88
	NCEP/NCAR-1	0.07	−5.55	120.12	88.11
Summer	ERA-Interim	0.57	27.80	187.92	154.01
	JRA-55	0.66	1.86	120.62	95.39
	NCEP/NCAR-1	0.12	1.99	211.08	170.28
Autumn	ERA-Interim	0.66	10.38	87.10	67.36
	JRA-55	0.70	8.49	83.21	62.20
	NCEP/NCAR-1	0.05	−14.92	171.11	128.61
Winter	ERA-Interim	0.49	109.77	36.03	31.26
	JRA-55	0.17	209.67	65.95	58.16
	NCEP/NCAR-1	0.05	16.03	29.43	21.06

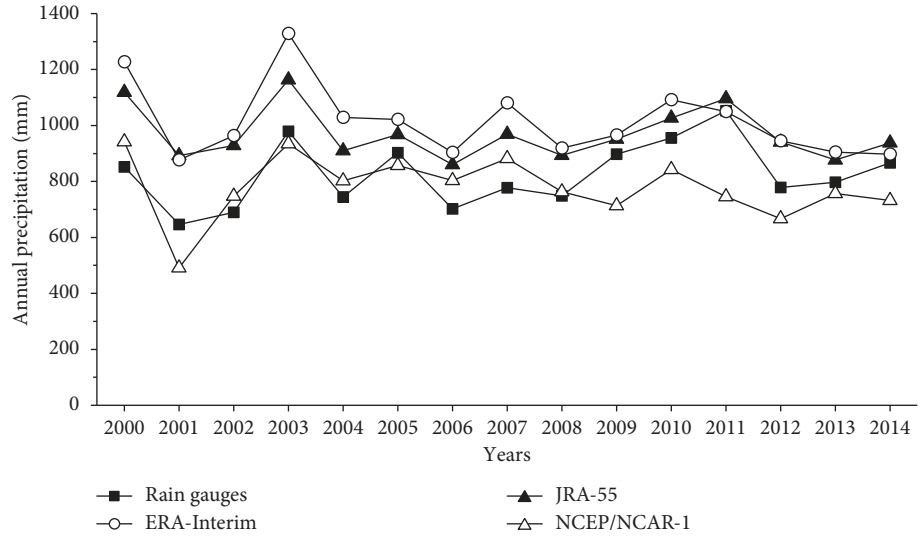

Figure 6: The line chart of regional average annual precipitation from rain gauges and the three reanalysis datasets.

Table 4: CC, BIAS, RMSE, and MAE between three reanalysis precipitation datasets and gauged rainfall at annual scale over the Qinling-Daba Mountains, China (all products passed the significance test at the 99% confidence level).

Index	ERA-Interim	JRA-55	NCEP/NCAR-1
CC	0.54	0.56	−0.19
BIAS	21.78	16.57	−6.31
RMSE	298.21	265.40	437.87
MAE	243.93	214.38	340.83

total migration distances of gauge, ERA-Interim, JRA-55, and NCEP/NCAR-1 were determined to be 188.8, 177.9, 159.2, and 296.1 km, respectively. The migration distance of JRA-55 was closest to the gauge precipitation, followed by ERA-Interim, while NCEP/NCAR-1 had the largest deviations from the gauges.

5. Discussion

5.1. Poor Performance in Winter. In terms of time, all three reanalysis precipitation datasets showed poor performance in winter on a seasonal and monthly scale. Standard Chinese rain gauges lack windproof and automatic heating devices; the solid precipitation measured is artificially melted into water immediately after the snow events. Considering the complexity of mountainous areas such as QDM, the interference by wind may cause only half of the actual precipitation to be represented by observed solid precipitation in rain gauges without a windproof device [57]. Moreover, the wetting losses caused by snow probably have an impact on the observation results in winter [58]. Large underestimations probably exist in observed winter precipitation and most likely prevent reanalysis datasets from agreeing well with the observation data. The performance of different precipitation products needs to further evaluate by measuring more winter precipitation by more windproofed weighted rain gauges.

5.2. Poor Performance at Wudu Station and Huashan Station. The three datasets evaluated in this work display bigger errors and larger deviations at Wudu station than the other stations, for which the complex terrain may be responsible. Wudu station is located in the Bailongjiang River valley with

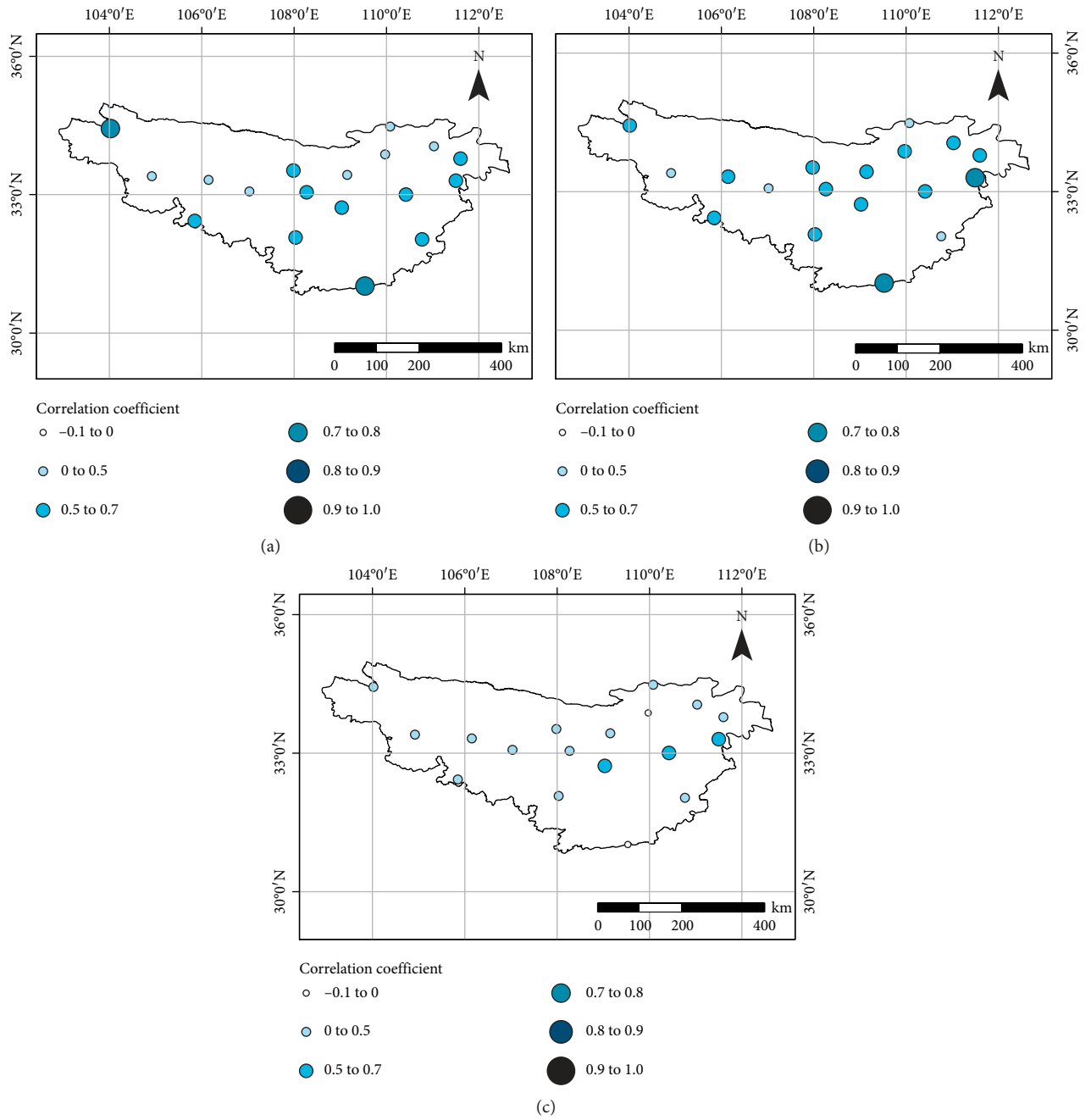

Figure 7: Correlation coefficient at each gauge over the Qinling-Daba Mountains for annual precipitation between (a) ERA-Interim and gauges, (b) JRA-55 and gauges, and (c) NCEP/NCAR-1 and gauges.

an altitude of 1079 m a.s.l., while the mountains on both sides are all above this elevation, and the peak of the mountains are above 2500 m a.s.l. Although the concave terrain allows the rain gauge at Wudu station to obtain accurate rainfall in the valley, it cannot reflect the true precipitation information in the surrounding areas to some extent. Some precipitation recorded at Wudu station was probably caused by local convection, but not over a large range. On the other hand, the difference between the actual altitude and the altitude in different reanalysis data probably contributes to the relatively large errors at Wudu station, where the complex terrain cannot be represented by coarse resolution reanalysis data.

The elevation of Huashan station is 2064 m a.s.l., which almost reaches the elevation of peak of Huashan Mountain (2154 m a.s.l.). The three reanalysis precipitation datasets underestimated the precipitation at Huashan station at the same time, which also can be explained by the large difference between the actual altitude and the altitude in different reanalysis data. This also indicates that there are precipitation gradients around Huashan stations, although they are difficult to be detected in current in situ observation

Table 5: The PDs and PPDs between ERA-Interim, JRA-55, and NCEP/NCAR-1 and observed precipitation for the wet years.

Reanalysis	ERA-Interim	JRA-55	NCEP/NCAR-1
Absolute precipitation difference (mm)			
2000	405.25	259.75	94.72
2003	371.56	192.93	−55.51
2005	125.74	60.4	−48.49
2009	103.6	69.75	−121.62
2010	178.22	97.56	−43.38
2011	39.93	68.77	−242.83
2014	52.86	83.53	−84.66
Percentage of PD (%)			
2000	46.18	29.6	10.79
2003	37.61	19.53	−5.62
2005	13.76	6.61	−5.31
2009	11.94	8.04	−14.01
2010	19.32	10.58	−4.7
2011	3.99	6.88	−24.28
2014	6.29	9.93	−10.07

Table 6: The PDs and PPDs between ERA-Interim, JRA-55, and NCEP/NCAR-1 and observed precipitation for the dry years.

Reanalysis	ERA-Interim	JRA-55	NCEP/NCAR-1
The absolute precipitation difference (mm)			
2001	234.99	233.97	−170.66
2002	269.71	215.85	40.56
2004	283.36	135.59	39.84
2006	196.41	143.75	85.85
2007	320.53	183.57	92.53
2008	167.6	118.2	−9.86
2012	187.36	159.27	−72.32
2013	148.97	119.31	36.18
Percentage of PD (%)			
2001	35.4	35.25	−25.71
2002	37.42	29.95	5.63
2004	36.4	17.42	5.12
2006	27.42	20.07	11.98
2007	39.62	22.69	11.44
2008	21.2	14.95	−1.25
2012	24.89	21.16	−9.61
2013	20.03	16.05	4.87

and satellite precipitation products. More intense in situ precipitation observation network will help to obtain the local precipitation gradients.

5.3. Reasons for Different Performance of Three Products. It needs to note that various reanalysis datasets may have varied performance on different scales and for each evaluation index. Harada et al. [38] found that JRA-55 had better correlation coefficients than NCEP/NCAR-1 in Eurasia and North America, which is in line with our research results. Wang and Zeng [59] found GLDAS has the best overall performance for daily and monthly precipitation, while ERA-40 and MERRA have the highest CCs. In this study, although the BIAS values of NCEP/NCAR-1 were good, the other indices of NCEP/NCAR-1 are relatively poor. The reasons include the following:

ERA-Interim and JRA-55 merged precipitation data from observed stations, while no rain observations were included for assimilation of the NCEP/NCAR-1 model. However, how many and which stations in the QDM were involved in ERA-Interim and JRA-55 are difficult to obtain and cannot be excluded in the evaluation. It seems unfair to compare ERA-Interim, JRA-55, and NCEP/NCAR-1 by the same observation data. On the other hand, the coarsest spatial resolution may be another reason for the poor performance of NCEP/NCAR-1. Meanwhile, the advantages of the four-dimensional variational analysis over three-dimensional variational analysis model is potentially one of reasons why ERA-Interim and JRA-55 showed higher agreement than NCEP/NCAR-1 [42], which has also been proven in previous studies [60, 61]. Moreover, due to the differences in the original resolution of different reanalysis data, the interpolation method likely has some impact on the evaluation.

It should also be noted that the observed precipitation also probably has some uncertainty. The general problem of representativeness is particularly acute in the measurement of precipitation, and precipitation measurements are particularly sensitive to exposure, wind, and topography. Although both the meteorological stations are observed with the manually standard process in the standard field with grass land cover, the local factors such as terrain and wind are still different to considered and corrected. Many different studies [62–64], among many, have concluded that automated gauges have many errors associated with them, among which some errors as high as 80% under extremely detrimental conditions. There is a whole entire field of quality controlling gauge data to further quality control radar-derived rain rates. Therefore, these flaws should be fixed in future studies on the evaluation of multiple precipitation datasets, including use of potentially more effective hydrological models.

5.4. Comparisons with Previous Study in QDM. Based on this study and Wang's previous study [27] on satellite-based precipitation datasets in QDM, ITPCAS has the highest accuracy among satellite precipitation datasets, such as CMORPH, GPCP-2, and GPCC compared against the rain-gauge observations. It also has the better accuracy with higher CC, lower BIAS, RMSE, and MAE than the three reanalysis precipitation products in this study. The main reason is probably because ITPCAS integrate more rain gauge observation data, which also used for the baseline of the evaluation. Thus, it was excluded in the evaluation. This study indicates that high precision precipitation datasets, including ERA-Interim and JRA-55 in this study, can be applied into hydrological models, and the applicability and adaptability of different precipitation datasets provide an important basis for hydrometeorological simulation and other applications in the QDM, which will also help to understand the water cycle in the whole Tibetan Plateau.

6. Conclusions

QDM is a unique region where precipitation can significantly be impacted by the terrain which has serious impacts

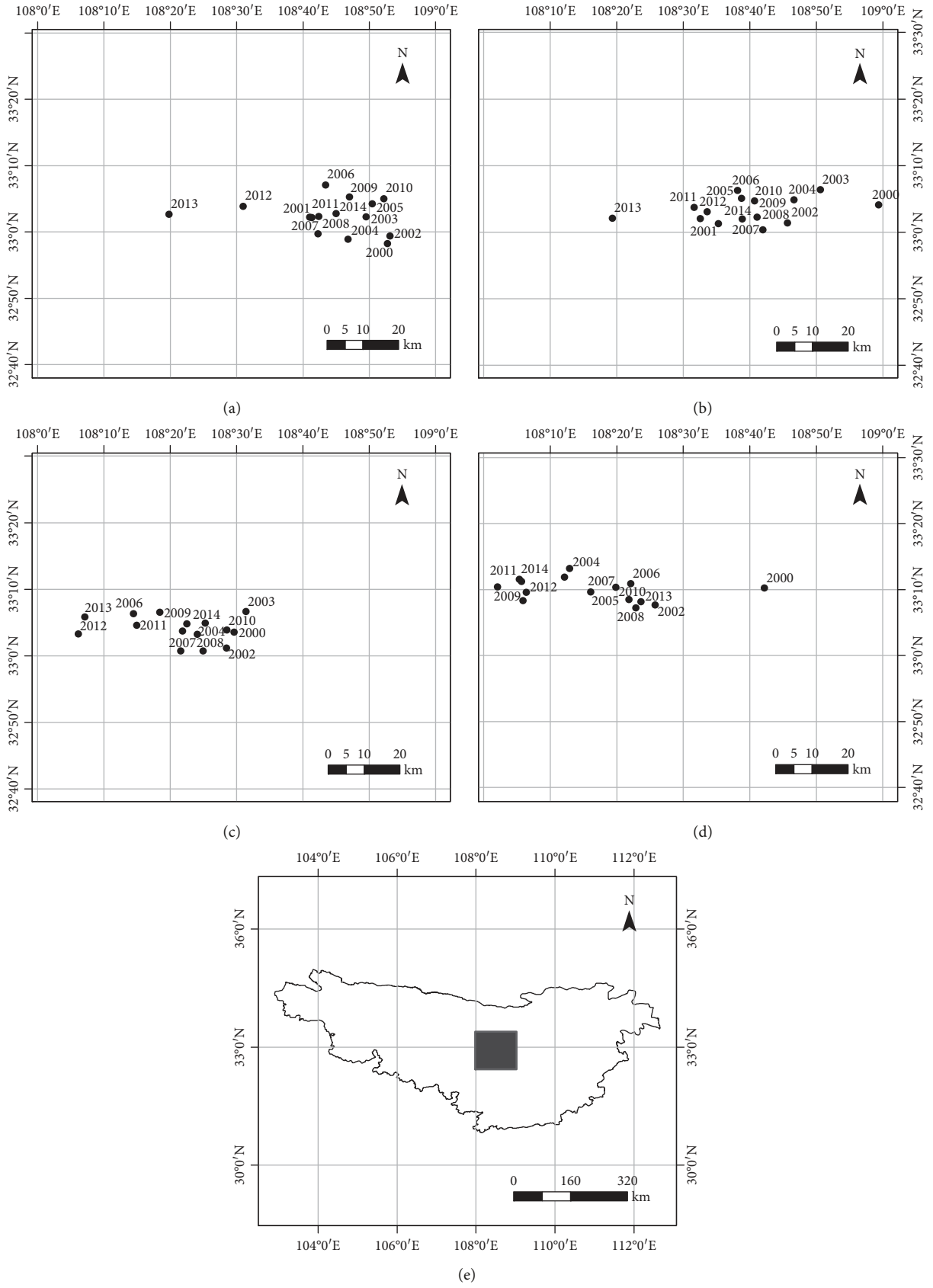

Figure 8: The precipitation centroids over the Qinling-Daba Mountains during 2000 to 2014 of (a) rain gauge, (b) ERA-Interim, (c) JRA-55, and (d) NCEP/NCAR-1, and (e) the black box represents the data range in a–d.

Table 7: The migration distance (km) of precipitation centroid of gauge and precipitation products.

Year	Gauge	ERA-Interim	JRA-55	NCEP/NCAR-1
2000				
2001	19.6	40.3	7.2	55.7
2002	19.6	19.1	8.6	30.3
2003	8.9	12.0	11.1	22.5
2004	7.6	6.8	13.0	2.8
2005	11.4	12.2	10.7	12.3
2006	12.2	2.4	6.2	3.6
2007	8.9	8.0	15.2	9.6
2008	4.9	5.7	5.2	9.2
2009	12.6	3.8	7.4	25.7
2010	8.1	4.5	10.4	28.6
2011	17.7	14.2	21.2	33.8
2012	16.4	3.5	14.0	7.1
2013	17.5	20.6	5.0	26.5
2014	39.2	24.8	24.1	28.4
Sum	204.6	177.9	159.2	296.1

to the local community by environmental, ecological, and biological processes. Three reanalysis precipitation datasets, including ERA-Interim, JRA-55, and NCEP/NCAR-1, were evaluated over the QDM against rain gauge data from 2000 to 2014 on monthly, seasonal, and annual scales. Based on all results, some conclusions can be made:

Overall, the performance of ERA-Interim is close to that of JRA-55 with higher CC above 0.5 and lower RMSE less than 50 mm in monthly scale, while NCEP/NCAR-1 has the worst performance on a monthly scale and annual scale. However, the NCEP/NCAR-1 has the least BIAS with the observed precipitation in an annual scale in QDM.

All reanalysis datasets performed better in spring, summer, and autumn than in winter. JRA-55 had a better agreement with rain gauge data in summer and autumn, while ERA-Interim exhibited a higher agreement in spring and winter in QDM.

The advantages of involving more precipitation observation stations are probably the main reason of the different performance of three precipitation reanalysis products, and the benefit of a four-dimensional variational analysis model over a three-dimensional variational analysis model may be another reason.

The evaluation on different precipitation products is very important to understanding the spatial-temporal distribution of precipitation in QDM, which is critical to simulation the hydrological processes and water resource management in QDM, where is the main water source of Xian city. Enhancing the precipitation measuring accuracy, especially in winter, and increasing the measuring stations are still needed to further evaluation the different precipitation products in QDM.

Data Availability

All relevant data can be obtained from the following links. ERA-Interim can be obtained from https://apps.ecmwf.int/datasets/, JRA-55 data from https://jra.kishou.go.jp, NCEP/NCAR-1 from https://www.esrl.noaa.gov/, ground-based measurements from the National Meteorological Information Center of the China Meteorological Administration https://data.cma.cn/, and DEM data from http://srtm.csi.cgiar.org.

Conflicts of Interest

The authors declare that they have no conflicts of interest.

Acknowledgments

This work was supported by the National Key Research and Development Plan (2017YFC1502501) and China National Natural Science Foundation (nos. 41671056 and 41730751).

References

[1] Y. Tian, C. D. Peters-Lidard, B. J. Choudhury, and M. Garcia, "Multitemporal analysis of TRMM-based satellite precipitation products for land data assimilation applications," *Journal of Hydrometeorology*, vol. 8, no. 6, pp. 1165–1183, 2007.

[2] Z. Duan, J. Liu, Y. Tuo, G. Chiogna, and M. Disse, "Evaluation of eight high spatial resolution gridded precipitation products in Adige Basin (Italy) at multiple temporal and spatial scales," *Science of the Total Environment*, vol. 573, pp. 1536–1553, 2016.

[3] M. R. P. Sapiano and P. A. Arkin, "An intercomparison and validation of high-resolution satellite precipitation estimates with 3-hourly gauge data," *Journal of Hydrometeorology*, vol. 10, no. 1, pp. 149–166, 2009.

[4] C. Kidd and V. Levizzani, "Status of satellite precipitation retrievals," *Hydrology and Earth System Sciences*, vol. 15, no. 4, pp. 1109–1116, 2011.

[5] A. Behrangi, B. Khakbaz, T. C. Jaw, A. AghaKouchak, K. Hsu, and S. Sorooshian, "Hydrologic evaluation of satellite precipitation products over a mid-size basin," *Journal of Hydrology*, vol. 397, no. 3-4, pp. 225–237, 2011.

[6] F. Su, Y. Hong, and D. P. Lettenmaier, "Evaluation of TRMM multisatellite precipitation analysis (TMPA) and its utility in hydrologic prediction in the La Plata basin," *Journal of Hydrometeorology*, vol. 9, no. 4, pp. 622–640, 2008.

[7] L. A. Blacutt, D. L. Herdies, L. G. G. de Gonçalves, D. A. Vila, and M. Andrade, "Precipitation comparison for the CFSR, MERRA, TRMM3B42 and combined scheme datasets in Bolivia," *Atmospheric Research*, vol. 163, pp. 117–131, 2015.

[8] T. Zhao, C. Fu, Z. Ke, and W. Guo, "Global atmosphere reanalysis datasets: current status and recent advances," *Advances in Earth Science*, vol. 25, pp. 242–254, 2010.

[9] S. Jiang, L. Ren, Y. Hong et al., "Comprehensive evaluation of multi-satellite precipitation products with a dense rain gauge network and optimally merging their simulated hydrological flows using the Bayesian model averaging method," *Journal of Hydrology*, vol. 452-453, pp. 213–225, 2012.

[10] H. Feidas, "Validation of satellite rainfall products over Greece," *Theoretical and Applied Climatology*, vol. 99, no. 1-2, pp. 193–216, 2009.

[11] M. Darand, J. Amanollahi, and S. Zandkarimi, "Evaluation of the performance of TRMM multi-satellite precipitation analysis (TMPA) estimation over Iran," *Atmospheric Research*, vol. 190, pp. 121–127, 2017.

[12] M. L. M. Scheel, M. Rohrer, C. Huggel, D. Santos Villar, E. Silvestre, and G. J. Huffman, "Evaluation of TRMM Multi-satellite Precipitation Analysis (TMPA) performance in the

central Andes region and its dependency on spatial and temporal resolution," *Hydrology and Earth System Sciences*, vol. 15, no. 8, pp. 2649–2663, 2011.

[13] S.-h. Jiang, M. Zhou, L.-l. Ren, X.-r. Cheng, and P.-j. Zhang, "Evaluation of latest TMPA and CMORPH satellite precipitation products over Yellow river basin," *Water Science and Engineering*, vol. 9, no. 2, pp. 87–96, 2016.

[14] T. C. Liechti, J. P. Matos, J.-L. Boillat, and A. J. Schleiss, "Comparison and evaluation of satellite derived precipitation products for hydrological modeling of the Zambezi river basin," *Hydrology and Earth System Sciences*, vol. 16, no. 2, pp. 489–500, 2012.

[15] Y. Tian and C. D. Peters-Lidard, "A global map of uncertainties in satellite-based precipitation measurements," *Geophysical Research Letters*, vol. 37, no. 24, pp. 701–719, 2010.

[16] M. R. P. Sapiano, D. B. Stephenson, H. J. Grubb, and P. A. Arkin, "Diagnosis of variability and trends in a global precipitation dataset using a physically motivated statistical model," *Journal of Climate*, vol. 19, no. 17, pp. 4154–4166, 2006.

[17] J. E. Janowiak, A. Gruber, C. R. Kondragunta, R. E. Livezey, and G. J. Huffman, "A comparison of the NCEP-NCAR reanalysis precipitation and the GPCP rain gauge-satellite combined dataset with observational error considerations," *Journal of Climate*, vol. 11, no. 11, pp. 2960–2979, 1998.

[18] G. J. Huffman, R. F. Adler, P. Arkin et al., "The global precipitation climatology project (GPCP) combined precipitation dataset," *Bulletin of the American Meteorological Society*, vol. 78, no. 1, pp. 5–20, 1997.

[19] C. Kummerow, J. Simpson, O. Thiele et al., "The status of the Tropical Rainfall Measuring Mission (TRMM) after two years in orbit," *Journal of Applied Meteorology*, vol. 39, no. 12, pp. 1965–1982, 2000.

[20] T. Zhao and C. Fu, "Preliminary comparison and analysis between ERA-40, NCEP-2 reanalysis and observations over China," *Climatic and Environmental Research*, vol. 11, pp. 14–32, 2006.

[21] L. Ma, T. Zhang, O. W. Frauenfeld, B. Ye, D. Yang, and D. Qin, "Evaluation of precipitation from the ERA-40, NCEP-1, and NCEP-2 reanalyses and CMAP-1, CMAP-2, and GPCP-2 with ground-based measurements in China," *Journal of Geophysical Research*, vol. 114, no. 9, article D09105, 2009.

[22] T. Zhao and A. Yatagai, "Evaluation of TRMM 3B42 product using a new gauge-based analysis of daily precipitation over China," *International Journal of Climatology*, vol. 34, no. 8, pp. 2749–2762, 2013.

[23] L. Cheng, R. Shen, C. Shi, L. Bai, and Y. Yang, "Evaluation and verification of CMORPH and TRMM 3B42 precipitation estimation products," *Meteorological Monthly*, vol. 40, pp. 1372–1379, 2014.

[24] S. Xu, Z. Niu, Y. Shen, and D. Kuang, "A research into the characters of CMORPH remote sensing precipitation error in China," *Remote Sensing Technology and Aplication*, vol. 29, pp. 189–194, 2014.

[25] T. Condom, P. Rau, and J. C. Espinoza, "Correction of TRMM 3B43 monthly precipitation data over the mountainous areas of Peru during the period 1998-2007," *Hydrological Processes*, vol. 25, no. 12, pp. 1924–1933, 2011.

[26] L. Ren, X. Wang, and Z. Zeng, "The accuracy evaluation of TRMM 3B42 precipitation data in Shaanxi Qinling-Daba mountains," *Journal of Shaanxi Normal University (Natural Science Edition)*, vol. 45, pp. 87–97, 2017.

[27] G. Wang, P. Zhang, L. Liang, and S. Zhang, "Evaluation of precipitation from CMORPH, GPCP-2, TRMM 3B43, GPCC, and ITPCAS with ground-based measurements in the Qinling-Daba mountains, China," *PLoS One*, vol. 12, no. 10, Article ID e0185147, 2017.

[28] L. Gao, K. Schulz, and M. Bernhardt, "Statistical downscaling of ERA-Interim forecast precipitation data in complex terrain using lasso algorithm," *Advances in Meteorology*, vol. 2014, Article ID 472741, 16 pages, 2014.

[29] A. K. Betts, M. Kohler, and Y. Zhang, "Comparison of river basin hydrometeorology in ERA-Interim and ERA-40 reanalysis with observations," *Journal of Geophysical Research Atmospheres*, vol. 114, no. 2, 2009.

[30] W. Yanase, H. Niino, S.-i.I. Watanabe et al., "Climatology of polar lows over the Sea of Japan using the JRA-55 reanalysis," *Journal of Climate*, vol. 29, no. 2, 2015.

[31] N. Kayaba, T. Yamada, S. Hayashi et al., "Dynamical regional downscaling using the JRA-55 reanalysis (dsjra-55)," *Sola*, vol. 12, pp. 1–5, 2016.

[32] H. Bai, *The Response of Forest Vegetation to Environment Changes in Qingling-Daba Mountainous Area*, China Science Publishing & Media Ltd., Beijing, China, 1st edition, 2014.

[33] X. Liu, Y. Pan, X. Zhu, and S. Li, "Spatiotemporal variation of vegetation coverage in Qinling-Daba mountains in relation to environmental factors," *Acta Oceanologica Sinica*, vol. 70, pp. 705–716, 2015.

[34] Q. Zhou, J. Bian, and J. Zheng, "Variation of air temperature and thermal resources in the northern and southern regions of the Qinling mountains from 1951 to 2009," *Acta Oceanologica Sinica*, vol. 66, pp. 1211–1218, 2011.

[35] H. Bai, X. Ma, X. Gao, and Q. Hou, "Variations in January temperature and 0 °C isothermal curve in Qinling mountains based on dem," *Acta Oceanologica Sinica*, vol. 67, pp. 1443–1450, 2012.

[36] D. P. Dee, S. M. Uppala, A. J. Simmons et al., "The ERA-Interim reanalysis: configuration and performance of the data assimilation system," *Quarterly Journal of the Royal Meteorological Society*, vol. 137, no. 656, pp. 553–597, 2011.

[37] M. B. Sylla, E. Coppola, L. Mariotti et al., "Multiyear simulation of the african climate using a regional climate model (REGCM3) with the high resolution era-interim reanalysis," *Climate Dynamics*, vol. 35, no. 1, pp. 231–247, 2009.

[38] Y. Harada, H. Kamahori, C. Kobayashi et al., "The JRA-55 reanalysis: representation of atmospheric circulation and climate variability," *Journal of the Meteorological Society of Japan. Ser. II*, vol. 94, no. 3, pp. 269–302, 2016.

[39] A. Ebita, S. Kobayashi, Y. Ota et al., "The Japanese 55-year reanalysis "JRA-55:" an interim report," *SOLA*, vol. 7, pp. 149–152, 2011.

[40] K. Onogi, J. Tsutsui, H. Koide et al., "The JRA-25 reanalysis," *Journal of the Meteorological Society of Japan. Ser. II*, vol. 85, no. 3, pp. 369–432, 2007.

[41] S. Kobayashi, Y. Ota, Y. Harada et al., "The JRA-55 reanalysis: general specifications and basic characteristics," *Journal of the Meteorological Society of Japan. Ser. II*, vol. 93, no. 1, pp. 5–48, 2015.

[42] E. Kalnay, M. Kanamitsu, R. Kistler et al., "The NCEP/NCAR 40-year reanalysis project," *Bulletin of the American Meteorological Society*, vol. 77, no. 3, pp. 437–471, 1996.

[43] I. Poccard, S. Janicot, and P. Camberlin, "Comparison of rainfall structures between NCEP/NCAR reanalyses and observed data over tropical Africa," *Climate Dynamics*, vol. 16, no. 12, pp. 897–915, 2000.

[44] National Meteorological bureau, *Criterion of Ground Meteorological Observation*, Meteorological Press, Beijing, China, 1979.

[45] Z. Li, D. Yang, and Y. Hong, "Multi-scale evaluation of high-resolution multi-sensor blended global precipitation products over the Yangtze river," *Journal of Hydrology*, vol. 500, pp. 157–169, 2013.

[46] Z. Hu, Y. Ni, H. Shao, G. Yin, Y. Yan, and C. Jia, "Applicability study of CFSR, ERA-Interim and MERRA precipitation estimates in Central Asia," *Arid land geography*, vol. 36, pp. 700–708, 2013.

[47] Z. Zhu, C. Shi, T. Zhang, C. Zhu, and X. Meng, "Applicability analysis of various reanalyzed land surface temperature datasets in China," *Journal of Glaciology and Geocryology*, vol. 37, no. 4, pp. 614–624, 2015.

[48] L. Sun, Z. Hao, J. Wang, I. Nistor, and O. Seidou, "Assessment and correction of TMPA products 3B42RT and 3B42v6," *Shuili Xuebao*, vol. 46, pp. 1135–1146, 2014.

[49] X. Zhang, Y. Wang, and Wang, *J. Statistics*, Tsinghua University Press, Beijing, China, 2012.

[50] J. Li and X. . e. Qi, *Principles of statistics*, Fudan University Press, Shanghai, China, 6th edition, 2014.

[51] F. Bellone and R. Cunningham, "All roads lead to center Laxton," *Journal of Economic Integration*, vol. 13, pp. 47–52, 1993.

[52] J. M. Grether and N. A. Mathys, "Is the world's economic center of gravity already in Asia?," *Area*, vol. 42, no. 1, pp. 47–50, 2010.

[53] D. Austin, "A new method for computing the mean center of population of the United States," *Professional Geographer*, vol. 58, no. 1, pp. 65–69, 2010.

[54] Z. Li, W. Guan, and W. Ke, "The regional gravity evolution of consumption, economy and population based on the multiple time scales in China," *Economic Geography*, vol. 34, pp. 7–14, 2014.

[55] S. Chen, L. Li, J. Li, and X. Liu, "Analysis of the temporal and spatial variation characteristics of precipitation in the Lancang river basin over the past 55 years," *Journal of Geo-information Science*, vol. 19, pp. 365–373, 2017.

[56] W. Wang, W. Zhang, W. Tan, and X. Wu, "Applicability analysis of TRMM 3B43 precipitation product concerning the spatial and temporal heterogeneity of precipitation: taking Hubei province as an example," *Geography and Geo-Information Science*, vol. 33, pp. 59–66, 2017.

[57] D. Yang, T. Jiang, Y. Zhang, and E. Kang, "Analysis and correction of errors in precipitation measurement at the head of Urumqi river, Tianshan," *Journal of Gaciology and Geocryology*, vol. 10, pp. 384–400, 1988.

[58] D. Yang, "A case study of the wetting loss experiments in the rain gauge," *Meteorological Monthly*, vol. 13, no. 7, pp. 16–18, 1987.

[59] A. Wang and X. Zeng, "Evaluation of multireanalysis products with in situ observations over the Tibetan plateau," *Journal of Geophysical Research Atmospheres*, vol. 117, no. 5, 2012.

[60] C. T. Dhanya and G. Villarini, "An investigation of predictability dynamics of temperature and precipitation in reanalysis datasets over the continental United States," *Atmospheric Research*, vol. 183, pp. 341–350, 2016.

[61] G. Fu, S. P. Charles, B. Timbal, B. Jovanovic, and F. Ouyang, "Comparison of NCEP-NCAR and ERA-interim over Australia," *International Journal of Climatology*, vol. 36, no. 5, pp. 2345–2367, 2015.

[62] M. J. Simpson, A. Hirsch, K. Grempler, and A. Lupo, "The importance of choosing precipitation datasets," *Hydrological Processes*, vol. 31, no. 25, pp. 4600–4612, 2017.

[63] E. Habib, W. F. Krajewski, and A. Kruger, "Sampling errors of tipping-bucket rain gauge measurements," *Journal of Hydrologic Engineering*, vol. 6, no. 2, pp. 159–166, 2001.

[64] Y. Qi, S. Martinaitis, J. Zhang, and S. Cocks, "A real-time automated quality control of hourly rain gauge data based on multiple sensors in MRMS system," *Journal of Hydrometeorology*, vol. 17, no. 6, pp. 1675–1691, 2016.